Microchim Acta (2015) 182:1247–1254
DOI 10.1007/s00604-015-1445-4

ORIGINAL PAPER

Determination of 4-aminophenylarsonic acid using a glassy carbon electrode modified with an ionic liquid and carbon nanohorns

Hong Dai · Lingshan Gong · Shuangyan Lu · Qingrong Zhang · Yilin Li · Shupei Zhang · Guifang Xu · Xiuhua Li · Yanyu Lin · Guonan Chen

Received: 14 August 2014 / Accepted: 5 January 2015 / Published online: 14 January 2015

Abstract We have developed a sensor for 4-aminophenylarsonic acid (4-APhAA) by coating a glassy carbon electrode (GCE) with a composite prepared from an ionic liquid and dahlia-like carbon nanohorns (CNHs). The good electric conductivity, large surface area and high pore volume of the CNHs, and the synergistic action of the ionic liquid (which is a good dispersant with excellent ion conductivity) result in efficient electrocatalysis towards oxidation of 4-APhAA. The effect was investigated by various electrochemical methods, and the electron transfer coefficient, diffusion coefficient, standard heterogeneous rate constant and thermodynamic activation energy were determined. The response range of 4-APhAA was evaluated using an i-t plot. If operated at a working voltage of 900 mV (vs Ag/AgCl), the sensor responds to 4-APhAA over the 0.5 μM to 3.5 M concentration range.

Keywords 4-aminophenylarsonic acid · Carbon nanohorns · Ionic liquid · Electrochemistry

Electronic supplementary material The online version of this article (doi:10.1007/s00604-015-1445-4) contains supplementary material, which is available to authorized users.

H. Dai (✉) · L. Gong · S. Lu · Q. Zhang · Y. Li · S. Zhang · G. Xu · X. Li · Y. Lin
College of Chemistry and Chemical Engineering, Fujian Normal University, Fuzhou, Fujian 350108, China
e-mail: dhong@fjnu.edu.cn

Y. Lin · G. Chen
Ministry of Education Key Laboratory of Analysis and Detection for Food Safety, and Department of Chemistry, Fuzhou University, Fuzhou, Fujian 350002, China

Introduction

Carbon nanohorn (CNH) is a top sealed conical carbon nanomaterial with the diameter of conical bottom 2–5 nm, height of 40–50 nm and cone angle of approximately 20° [1]. In addition, CNHs of high purity and high yield can be synthesized by CO_2 laser ablation of graphite as a carbon source under Ar atmosphere at room temperature [1]. CNHs have many advantages over other carbon nanomaterials. Firstly, aggregated cluster structure, dahlia-like carbon nanohorns, with thousands of outward horns perform many excellent properties, such as porous offered more sites to electro-active substances, admirable conductivity caused by center emitting horns, supercapacity with large specific surface area etc. [1]. Furthermore, a metal-free method of synthesis can produce highly pure material without purification and avoids interference [2], which was disputed among CNTs [3]. In addition, no toxicity was reported in various studies [4]. Due to these striking features, CNHs have attracted great interest with respect to potential applications, such as biomedicine, electrochemistry [5,6], supercapacitors [7], gas storage [8] and catalyst support [9]. For example, Bekarova et al. reported that a CNH-based sensing platform had a more sensitive response to fibrinogen than one based on MWCNTs [10]. Nevertheless, application of CNHs in electrochemistry is still limited and the potential applications await further exploration [11]. As is well known, ionic liquid (IL) possesses many unique physicochemical properties, for example a high ionic conductivity, low toxicity, wide electrochemical window, and good thermal stability [12]. Functionalization could further enhance the capabilities of ionic liquid; functionalized IL exhibits the merits of both the functionalized reagent and the original ionic liquid, such as improved nanomaterial

dispersibility, enhanced thermal stability, distinct mechanical properties and ionic conductivity. Furthermore, functionalized IL also facilitates application in biosensing [13,14]. Owing to their unique capabilities, IL have received much attention and are employed in various fields. For example, IL have proved to be an excellent stabilizer and modifier in the synthesis and functionalization of many nanomaterials, such as carbon nanomaterials and noble metal nanoparticles [15,16]. With the modification of IL, the mixture not only had the properties of nanomaterials, but also displayed better conductivity, excellent hydrophilicity, and other structural properties, which have reciprocity with the π conjugation structure of some nanomaterials. In this report, the mixture of CNHs and IL was modified on the glassy carbon electrode (GCE), as a result, the modified layer was endowed with both the properties of the modified compositions, for instance large surface area, good conductivity, stability etc. [17].

Most of the sensors developed need to be exploited in practical applications in order to demonstrate their advantageous features. As a detection target, arsenic species attract much interest in analysis detections. In comparison with inorganic arsenic compounds, organic arsenic compounds have always been considered have lower toxicity, therefore, the applications of organic arsenic compounds is much wider. However, recent reports indicate that they may harm human health and environment, because of their ease of bioaccumulation and slow metabolism [18]. 4-aminophenylarsonic acid as a common organic arsenic compound is usually used as a feed additive for increasing the rate of weight gain, improving feed efficiency, and preventing and treating coccidial intestinal parasites [9]. Therefore, it can be taken up by plants and subsequently transferred into the human food chain [19]. This can lead to demyelination and gliosis of peripheral nerves and optic nerve, so there is a limit of addition and the allowable amount of addition is from 50 to 100 mg/kg [20]. Therefore, it is imperative to find a method for achieving the quantitative detection of 4-aminophenylarsonic acid. Up to now, there have been many methods for detecting 4-aminophenylarsonic acid [21,22], and many coupling technologies [19,23,24], for example ATR–FTIR, HPLC-MS. Compared to the above detection techniques, the electrochemical method shows more promise for in-situ and real-time detection, because of the simplicity of the instrument, quick test process and straightforward sample treatment. However, electrochemistry has not been used for the quantificational detection of 4-aminophenylarsonic acid.

Herein, a stable and easily structured electrochemical sensor modified with CNHs and carboxylic IL (CIL) was built to achieve the fast detection of 4-aminophenylarsonic acid. The sensor was evaluated using many electrochemical techniques, including cyclic voltammetry, linear sweep voltammetry and amperometric i-t Curve. Results obtained have shown that the modified layer of mixture composition had large surface area and charge capability, good conductivity and stability, wide linear response range and fast electrochemical response which is closely related to pH and temperature during the 4-aminophenylarsonic acid oxidation process. These excellent properties of the electrochemical sensor architecture proved the prominent detection platform for 4-aminophenylarsonic acid detection and its potential for applications to real sample analysis.

Experimental

Reagents

4-aminophenylarsonic acid was purchased from Aladdin Inc. (Shanghai, China). Methylimidazole was bought from HWRK Chem Co. (http://www.hwrkchemical.com/, Beijing, China). 4 $mg \cdot mL^{-1}$ homogeneous CNHs mixture was prepared by separating CNHs into N,N-dimethylformamide with vigorous shaking and sonication. CNHs were obtained by synthesis as outlined in our previous report [25]. Briefly, CNHs were gained from the evaporation of pure graphite rods by the direct current arc-discharge method, with the current held at 120 A, and a pressure of 400 Torr in CO_2 atm. 0.1 M phosphate buffer solution of varying pH was obtained by mixing 0.1 M Na_2HPO_4 and NaH_2PO_4 with pH meter. Other reagents were analytical reagents. The ultrapure water used to prepare solution was purified using a Water Purifier (http://www.instrument.com.cn/netshow/SH101210/, Sichuan Water Purifier Water treatment Equipment Co., Ltd., China) purification system.

Apparatus and electrodes

All electrochemical process was performed using a CHI760 Electrochemistry workstation (http://www.chinstr.com/_d1479.htm, Shanghai Chenghua Instrument Co., China) with a three electrode system consisting of a platinum auxiliary electrode, a Ag/AgCl reference electrode (sat. KCl) and a glassy carbon working electrode (GCE, φ=3 mm) or modified GCE. The pH values were confirmed with a PHS-3C exact digital pH meter (http://www.lei-ci.com/, Shanghai Leici Co. Ltd., China).

Prepared carboxylic ion liquid

Carboxylic IL (CIL) were synthesized using the following processes [26]. Briefly, 0.04 mol methylimidazole and 0.06 mol chloroacetic acid was mixed in 20 mL toluene and

refluxed for 24 h; then, recrystallization was used to gain higher purity Carboxylic IL.

Preparation of the glassy carbon electrode modified with ionic liquid and carbon nanohorns

A clean GCE was obtained by polishing with chamois leather with 0.3 and 0.05 μm alumina particles, then washing with ethanol and water in sequence and natural drying in air. As the schematic diagram shows, the electrode was modified as follows: first, 3 μL 4 mg·mL^{-1} CNHs dispersed by DMF were dripped onto the clean GCE. The modified electrode was then set under an infrared lamp to dry to produce CNHs/GCE. 3 μL 10 mg·mL^{-1} IL was then dripped onto the modified electrode again, which was set under the infrared lamp to dry, cooled down to room temperature and in order to produce IL-CNHs/GCE.

Results and discussion

Choice of materials

CNHs combined with IL possess unique physicochemical properties [12] and were hence chosen to construct the electrochemical sensor. The micro-morphology of CNHs is shown in Fig. S1 (Electronic Supplementary Material, ESM). In the figure evenly dispersed dahlia-like CNHs cluster with central emitting horns are clearly observed.

The properties of different electrodes modified with various composites were compared. The CVs of different electrodes with and without the modified layer are shown in Fig. 1a. As evident from Fig. 1a for the modified IL on GCE, both oxidation and reduction potentials of Fe $(CN)_6^{3-/4-}$ clearly turned negative, which might be because of the good conductivity of the IL and the decrease in interface resistance in electrochemical reactions. The coordination between electrons of CIL and the vacant orbital of Fe $(CN)_6^{3-/4-}$ decreased the diffusion resistance of Fe $(CN)_6^{3-/4-}$ arriving at the electrode interface, and thus lower energy was needed during electrochemical reaction process. Due to the large surface area and good electrical conductivity the modified CNH/GCE lead to magnification of the currents. Figure 1a also displayed that peak current and background current of IL-CNHs/GCE significantly increased when CNHs were added to the modified layer. With a mixture of CNHs and IL, there are synergistic effects in the modified layer, resulting in increased numbers of electrochemically active sites, increased effective electrode area and increased adsorption. The active areas of the electrodes were calculated using the slope of the linear relationship between the charge and the square roots of the scan time as measured using Chronocoulometry and shown in Fig. 1b. The linear relationship follows Anson equation [27]:

$$Q(t) = \frac{2nFAcD^{1/2}t^{1/2}}{\pi^{1/2}} + Q_{ads}$$

Where A is electrode area, F, c, D, n are the Faradic constant, concentration, diffusion coefficient and transferred electron number of detected object, respectively. For c=5 mM, n=1 and $D_{OX}=7.63\times10^{-6}$ cm^2·s^{-1} for K_3 [Fe(CN)$_6$] the electrode areas could be calculated to be 0.0773, 0.313, 0.498 cm^2 for IL/GCE, CNHs/GCE and IL-CNHs/GCE, respectively. The active area of structured sensor is much larger than the geometrical surface area of the bare GCE. As is well known, the thickness of the outer Helmholtz plane (OHP) plays a crucial role in electrode kinetics, where the electrochemical reactions occur. By introducing the IL functional CNHs composite onto the electrode interface, the nanocomposites could effectively extend the OHP of this sensing interface and accelerate the electrochemical reaction. Thus, this nanomaterial architecture design for biosensor might possess unique analytical properties.

The capacitance capability of the modified layer was evaluated by CVs of GCE and IL-CNHs/GCE in 1 M KCl as shown in Fig. 1c and corresponding values of were calculated according the equation [28]: $C_{CV}=i/(s\nu)$, where i, s, ν are average charge or discharge current (A), electrode area (cm^2) and scan rate (V/s), respectively. The C_{CV} of GCE and IL-CNHs/GCE were calculated to be 23.09 and 392.7 μF·cm^{-2}

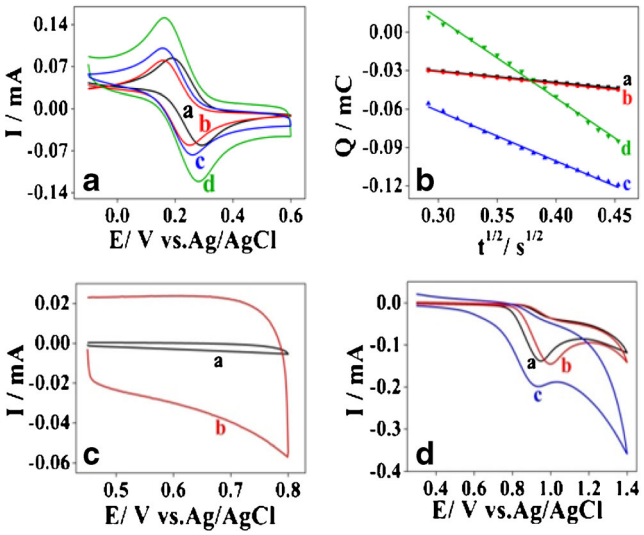

Fig. 1 **a** CVs of different electrodes (GCE (*a*), IL/GCE (*b*), CNHs/GCE (*c*),IL-CNHs/GCE (*d*)) in 5 mM K_3[Fe(CN)$_6$] at 0.1 V•s^{-1}. **b** Relationships (Q-t$^{1/2}$) of different electrodes (GCE (*a*), IL/GCE (*b*), CNHs/GCE (*c*),IL-CNHs/GCE (*d*)) in 5 mM K_3[Fe(CN)$_6$]. **c** CVs of GCE (*a*), IL-CNHs/GCE (*b*) in 1 M KCl at 1 V•s^{-1}. **d** CVs of different electrodes (GCE (*a*), IL/GCE (*b*), IL-CNHs/GCE (*c*)) in 0.1 M phosphate buffered solution containing 1 mM 4-aminophenylarsonic acid at 0.1 V•s^{-1}

respectively. In other words, capacitance of IL-CNHs/GCE was over 17 times that of GCE, meaning that CNHs having sp^2 conjugate structure and electrons moving through the whole conjugate system contributed to a high capacitance [29]. This capability indicates that CNHs can be used to as supercapacitor materials for designing sensors and other applications in the future. To further corroborate this characterization, electrochemical impedance spectroscopy was used to test the different electrodes, and a Bode-plot was produced to show the frequency dependent change in the phase angle in Fig. S2 (ESM). The nearly −90° phase angle represents a highly capacitive behavior [30], as confirmed by CV measurements.

The modified layer was coated onto an electrode to create a sensitive sensor for the quantificational detection of 4-aminophenylarsonic acid. Corresponding electrochemical behaviors of 4-aminophenylarsonic acid on different electrodes are shown in Fig. 1d. The current of 4-aminophenylarsonic acid on IL/GCE was a slightly higher than that of GCE, which may contribute to good conductivity and hydrophilicity and the large electrode area of IL/GCE. In addition, increases in current response also contributed to the existence of hydrogen bonds between the carboxyl group of CIL and the amino group of 4-aminophenylarsonic acid. Because the zwitterionic form of 4-aminophenylarsonic acid is predominant the electrostatic repulsion between rich electrons CIL and –HAsO3- hinder the target molecules to reach the electrode interface. As a result of this the electrochemical oxidation peak potential of 4-aminophenylarsonic acid on IL/GCE is slightly moved positive. It should be noticed that the current for 4-aminophenylarsonic acid rapidly increased and the potential of 4-aminophenylarsonic acid became more negative, with modified CNHs. This is due to the excellent properties of CNHs, such as large surface area, good conductivity, large absorption and prominent synergistic effect of CNHs and IL. Therefore, CNHs combined with IL could be used to create sensitive sensors for analysis detection of the target.

Diffusion coefficient of 4-aminophenylarsonic acid

The effect of scan rate on the oxidation process of 4-aminophenylarsonic acid was investigated. CVs in Fig. 2 were obtained by scanning 4.5 mM 4-aminophenylarsonic acid with different scan rates. In Fig. 2a, the oxidation peak currents and potentials of 4-aminophenylarsonic acid increased as scan rate increased. The corresponding relationship between oxidation peak potentials and the natural logarithm of scan rates was also investigated and was in accordance with the equation which follows [31]:

$$E_{pa} = E^0 + \frac{RT}{\alpha nF}\ln\frac{RTk^0}{\alpha nF} + \frac{RT}{\alpha nF}\ln\nu$$

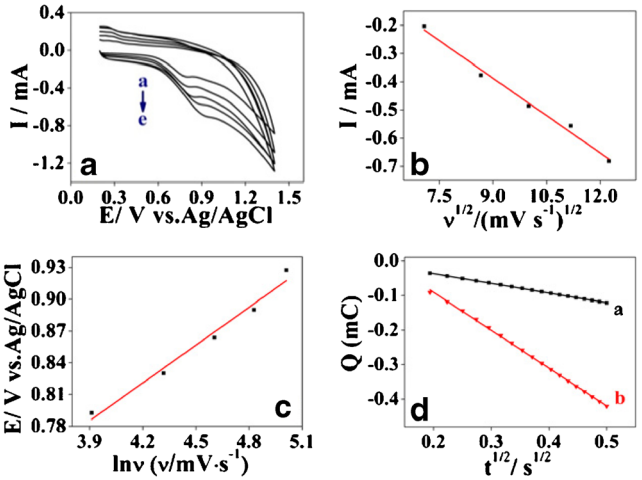

Fig. 2 **a** CVs of IL-CNHs/GCE in 4.5 mM 4-aminophenylarsonic acid at 0.1 M phosphate buffered solution with different scan rates, scan rates from a to e were 50, 75, 100, 125, 150 mV•s^{-1}. **b** Corresponding relationship between oxidation peak currents and square roots of scan rates. **c** Corresponding relationship between oxidation peak potentials and natural logarithm of scan rates. **d** Relationships (Q-$t^{1/2}$) of GCE (*a*), IL-CNHs/GCE (*b*) in 1 mM 4-aminophenylarsonic acid

Where α is the electron transfer coefficient, k^0 is the heterogeneous rate constant, ν is scan rate, and the values selected for R, T and F were 8.314 J·(mol·K)$^{-1}$, 298 K, 96,500 C·mol^{-1} respectively. For the total irreversible electrochemical reaction, the value of α is 0.5. The number of transferred electrons n=1 of electro-oxidation 4-aminophenylarsonic acid was derived from the slope of Ep-lnν in Fig. 2c. The result allows us to speculate on the mechanism of the 4-aminophenylarsonic acid oxidation process, as it was an electron oxidation process, so it should be that the amino group of 4-aminophenylarsonic acid was oxidized. The corresponding oxidation process is shown in the schematic diagram. As expected, this oxidation process was similar to the oxidation of the amino groups of p-aminobenzene sulfonic acid and p-phenylenediamine [32,33]. The final product looked like an excited molecule, while the conjugated structure provided stability. The two molecules produced may combine to form a more stable dipolymer as a product.

The good linear relation between oxidation peak currents and square roots of scan rates indicates that electrochemical oxidation of 4-aminophenylarsonic acid on IL-CNHs/GCE was a typical diffusion controlling process. The diffusion coefficient of 4-aminophenylarsonic acid was calculated using the following equation:

$$Q(t) = \frac{2nFAcD^{1/2}t^{1/2}}{\pi^{1/2}} + Q_{ads}$$

Where A=0.498 cm^2, c is 4.5 mM, n=1, and D is calculated to be 2.5×10^{-5} $cm^2\cdot s^{-1}$, indicating a very fast diffusion rate.

Effect of pH

Figure 3 shows the effect of pH on the electrochemical oxidation of 4-aminophenylarsonic acid in buffer solution with different pH values. With the pH value gradually increased, the corresponding oxidation peak potential gradually decreased, in accordance with the following equation:

$$E_p(V) = -0.056pH + 1.36\left(R^2 = 0.9888\right)$$

The slope of 56 mV per pH approaches 57.6 mV per pH, which indicates that the number of transferred electrons was equal to the number of protons taking part in the reaction. In Fig. 4c, the electrochemical current increases with increasing pH until pH=7.0. When the pH exceeds a value of 7.0, the electrochemical current decreases. This is probably due to the fact that 4-aminophenylarsonic acid at this pH usually exists as a zwitterion. At higher and lower pH 4-aminophenylarsonic acid does not diffuse to the electrode to take part in the reaction. Thus, pH 7.0 was chosen as the best buffer solution pH for subsequent reactions.

Activation energy of 4-aminophenylarsonic acid

The Linear Sweep Voltammetry (LSV) shown in Fig. 4a and b shows the electrochemical oxidation process of 4-aminophenylarsonic acid on GCE (A) and IL-CNHs/GCE (B) respectively at different temperatures. With the increase in temperature, the corresponding current response amplified both GCE and IL-CNHs/GCE. Moreover, oxidation peak potential tended to negative, suggesting that oxidation of 4-aminophenylarsonic acid is preferred at higher temperature. The relationship between the natural logarithm of the oxidation peak currents and the reciprocal of temperature is also shown in Fig. 4, and a line of best fit acquired by use of the Arrhenius equation $\ln I = \frac{Ea}{RT} + \ln A$ gave the following results:

$$\ln I_a = -248.01/T - 0.0845(GCE)$$

$$\ln I_b = -151.13/T - 0.385(IL-CNHs/GCE)$$

From the equations above, combined with the Arrhenius equation, the activation energies of 4-aminophenylarsonic acid of GCE and IL-CNHs/GCE were calculated to be 2.062 and 1.256 $kJ \cdot mol^{-1}$. The lower activation energy of IL-CNHs/GCE shows that electrochemical oxidation of 4-aminophenylarsonic acid on IL-CNHs/GCE was easier than GCE [34], because molecules become active molecules more easily by needing less energy.

Heterogeneous catalytic rate constant k_h

An amperometric i-t Curve was used to evaluate the heterogeneous catalytic rate constant k_h, which is a dynamic constant for evaluating the catalytic rate of the solid modified layer for 4-aminophenylarsonic acid in this paper, using the relationship between I_C/I_L and $t^{1/2}$, according to the equation [35]:

$$I_C/I_L = \pi^{1/2}\gamma^{1/2} = \pi^{1/2}\left(k_h C t^{1/2}\right)$$

Where I_C is the catalytic current of 4-aminophenylarsonic acid at the modified electrode, I_L is the limited current of the blank solution (buffer solution), C is the concentration of 4-aminophenylarsonic acid and t is time elapsed (s). Using the slope of the I_C/I_L - $t^{1/2}$ plot presented in Fig. 5b, the value of k_h was calculated to be 4.12×10^5 $cm^3 \cdot mol^{-1} \cdot s^{-1}$, which is larger than the value given in the work of Jahan Bakhsh Raoof et al. [36], indicating that the electro-oxidation of 4-aminophenylarsonic acid had a fast catalytic rate.

Sensitivity, selectivity, reproducibility and stability

An amperometric i-t Curve was used to demonstrate the linear response range of 4-aminophenylarsonic acid by gradually adding standard solution to a 0.1 M phosphate buffer solution at 900 mV. Changes of current response with concentration were used for the quantitative analysis (see Fig. 5). The linear regression equation is: I (mA)=−19.1C (mM) −2.73 (R= 0.9975). The linear range was from 0.5 μM to 3.48 mM, crossing 5 orders of magnitude, thus displaying a broad linear

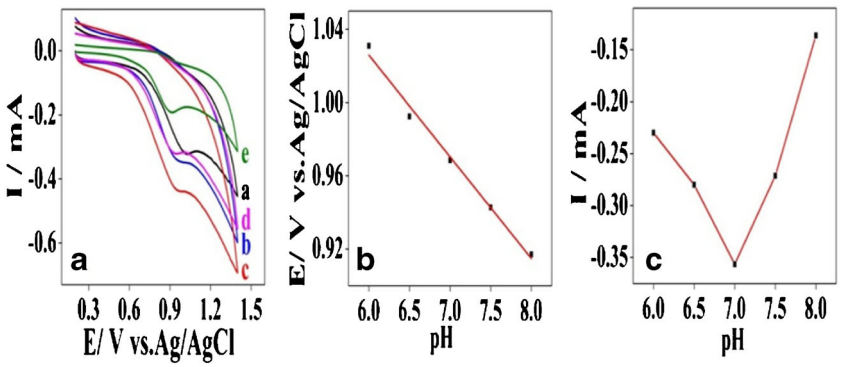

Fig. 3 **a** CVs of IL-CNHs/GCE in 4.5 mM 4-aminophenylarsonic acid at 0.1 M phosphate buffered solution with different pH, pH from a to e were 6, 6.5, 7, 7.5, 8, respectively. Corresponding changes of oxidation peak potentials **b** and peak currents **c** along with pH

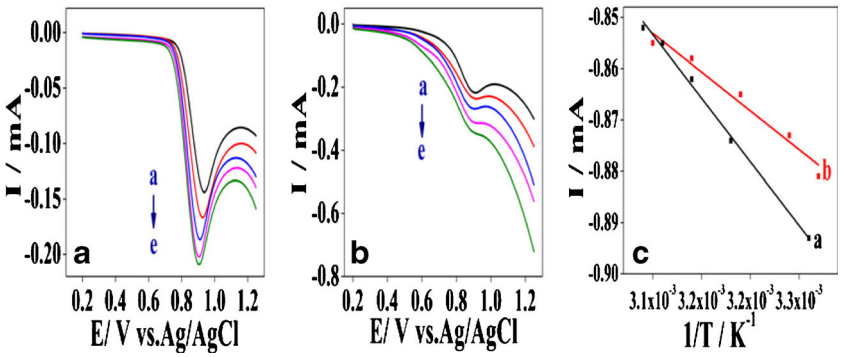

Fig. 4 LSVs of GCE (**a**) and IL-CNHs/GCE (**b**) in 4.5 mM 4-aminophenylarsonic acid concluding 0.1 M phosphate buffered solution pH=7.0 at different temperatures. (B) Corresponding relationships of GCE (*a*) and IL-CNHs/GCE (*b*) between currents and 1/T

range for the quantitative detection of 4-aminophenylarsonic acid. The detection limit of 4-aminophenylarsonic acid was 0.5 μM which is close to the value reported by Li when using LVSS-CE/UV [23]. A compilation of comparable methods for the determination 4-aminophenylarsonic acid is given in Table S1 (ESM). Due to separation and preconcentration other methods have very low limits of detection, but they also need complex preparation and large equipment which are disadvantageous for practical applications. For the practical application of this sensor, feed sample solution was tested with this sensor and a concentration of 91.46 $mg \cdot kg^{-1}$ was determined using a parallel test of four different modified electrodes (RSD=2.18 %). To investigate reproducibility, five different modified electrodes were tested at 3 days in sequence with an overall RSD of 3.79 %. Accuracy was checked by adding standard solution and the recovery rate found was 101.4 % (n=5). Some inorganic ions, for example, 200-fold concentrations of Na^+, K^+, Fe^{3+}, Ca^{2+}, Mg^{2+}, Al^{3+}, Zn^{2+}, SO_4^{2-}, Cl^-, NO_3^- and PO_4^{3-} had no influence on the determination of 4-aminophenylarsonic acid. A 50-fold excess of sucrose, glucose and starch, calcium gluconate, fibrin (Carboxymethylcellulose sodium), a 10-fold excess of bovine serum albumin and a 5-fold excess of 4-Hydrox-3-nitrobenzenearsonic acid had negligible effects on the precision of the determination of a 0.1 mM standard solution. The stability of the sensor prepared was tested by measuring the response of this sensor in 1 mM 4-aminophenylarsonic acid solution every 2 days. The results demonstrated that this sensor could maintain 91.9 % of its initial response after 12 days. Additionally, the relative standard deviation of five parallel measurements for 1 mM 4-aminophenylarsonic acid when using this sensor was 3.9 %. All these results suggest that ionic liquid and CNH-based sensors have good reproducibility and stability.

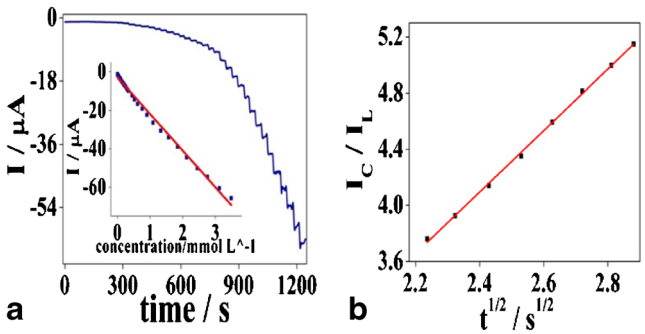

Fig. 5 **a** I-t curve of IL-CNHs/GCE in 0.1 M phosphate buffered solution pH 7.0 at 900 mV with incremental increase of 4-aminophenylarsonic acid concentration. Insets: the lower magnified concentration and corresponding relationship between currents and concentrations. **b** Linear relationship of I_C/I_L to $t^{0.5}$ of I-t curve

Conclusion

In summary, based on the excellent properties and synergistic effects of CNHs and IL, unique sensor architecture was built for the quantitative detection of 4-aminophenylarsonic acid. The electrochemical responses of the CNH modified electrode were superior to those of other sensors, indicating that CNHs may be a good modified material for improving the performance of sensing interfaces. In this report, both kinetic and thermodynamic parameters obtained by electrochemical methods showed that this sensor possesses many excellent characteristics. In particular the current response of 4-aminophenylarsonic acid is significantly enhanced and the sensor shows wide linear response range over five orders of magnitude. Owing to these excellent capabilities, target molecules could quickly react on this electrode interface which presented good sensitivity, selectivity, reproducibility and stability during the process of sensing.

Acknowledgments This project was financially supported by the National Nature Sciences Foundation of China (21205016), the National Science Foundation of Fujian Province (2011J05020), and the Education Department of Fujian Province (JA14071, JB14036, JA13068). Foundation of Fuzhou Science and Technology Bureau (2013-S-113) and Fujian Normal University outstanding young teacher research fund projects (fjsdjk2012068).

References

1. Zhu S, Xu G (2010) Single-walled carbon nanohorns and their applications. Nanoscale 2:2538–2549
2. Zhu S, Fan L, Liu X, Shi L, Li H, Han S, Xu G (2008) Determination of concentrated hydrogen peroxide at single-walled carbon nanohorn paste electrode. Electrochem Commun 10:695–698
3. Yang CM, Kim YJ, Endo M, Kanoh H, Yudasaka M, Iijima S, Kaneko K (2007) Nanowindow-regulated specific capacitance of supercapacitor electrodes of single-wall carbon nanohorns. J Am Chem Soc 129:20–21
4. Murata K, Kaneko K, Kanoh H, Kasuya D, Takahashi K, Kokai F, Yudasaka M, Iijima S (2002) Adsorption mechanism of supercritical hydrogen in internal and interstitial Nanospaces of single-wall carbon nanohorn assembly. J Phys Chem B 106:11132–11138
5. Zhang L, Lei J, Zhang J, Ding L, Ju H (2012) Amperometric detection of hypoxanthine and xanthine by enzymatic amplification using a gold nanoparticles-carbon nanohorn hybrid as the carrier. Analyst 137:3126–3131
6. Zhang J, Lei J, Xu C, Ding L, Ju H (2010) Carbon nanohorn sensitized electrochemical immunosensor for rapid detection of Microcystin-LR. Anal Chem 82:117–1122
7. Kumiko A, Tatsuya M, Sumio I, Toshinari I, Masako Y, Yoshikazu M, Kunihiro T (2008) Enhancement of in vivo anticancer effects of cisplatin by incorporation inside single-wall carbon nanohorns. ACS NANO 2:2057–2064
8. Kumiko A, Tatsuya M, Sumio I, Toshinari I, Masako Y, Yoshikazu M, Kunihiro T (2008) Enhancement of in vivo anticancer effects of cisplatin by incorporation inside single-wall carbon nanohorns. ACS NANO 2:2057–2064
9. Ojeda I, Garcinuno B, Moreno-Guzman M, Gonzalez-Cortes A, Yudasaka M, Iijima S, Langa F, Yanez-Sedeno P, Pingarron JM (2014) Carbon nanohorns as a scaffold for the construction of disposable electrochemical immunosensing platforms. Application to the determination of fibrinogen in human plasma and urine. Anal Chem 86:7749–7756
10. Bekyarova E, Hashimoto A, Yudasaka M, Hattori Y, Murata K, Kanoh H, Kasuya D, Iijima S, Kaneko K (2005) Palladium Nanoclusters deposited on single-walled carbon nanohorns. J Phys Chem B 109:3711–3714
11. Zhao Y, Li J, Ding Y, Guan L (2011) Single-walled carbon nanohorns coated with Fe2O3 as a superior anode material for lithium ion batteries. Chem Commun 47:7416–7418
12. Yang YC, Dong SW, Shen T, Jian CX, Chang HJ, Li Y, Zhou JX (2011) Amplified immunosensing based on ionic liquid-doped chitosan film as a matrix and Au nanoparticle decorated graphene nanosheets as labels. Electrochim Acta 56:6021–6025
13. Marcilla R, Alcaide F, Sardon H, Pomposo JA, Pozo-Gonzalo C, Mecerreyes D (2006) Tailor-made polymer electrolytes based upon ionic liquids and their application in all-plastic electrochromic devices. Electrochem Commun 8:482–488
14. Shen J, Hu Y, Li C, Qin C, Ye M (2009) Synthesis of amphiphilic graphene nanoplatelets. Small 5:82–85
15. Tollan CM, Marcilla R, Pomposo JA, Rodriguez J, Aizpurua J, Molina J, Mecerreyes D (2009) Irreversible thermochromic behavior in gold and silver nanorod/polymeric ionic liquid nanocomposite films. ACS Appl Mater Interfaces 1:348–352
16. Wu B, Hu D, Kuang Y, Liu B, Zhang X, Chen J (2009) Functionalization of carbon nanotubes by an ionic-liquid polymer: dispersion of Pt and PtRu nanoparticles on carbon nanotubes and their electrocatalytic oxidation of methanol. Angew Chem Int Ed 48:4751–4754
17. Brandao L, Boaventura M, Passeira C, Gattia DM, Marazzi R, Antisari MV, Mendes A (2011) An electrochemical impedance spectroscopy study of polymer electrolyte membrane fuel cells electrocatalyst single wall carbon nanohorns-supported. J Nanosci Nanotechnol 11:9016–9024
18. Sierra-Alvarez R, Cortinas I, Field JA (2010) Methanogenic inhibition by roxarsone (4-hydroxy-3-nitrophenylarsonic acid) and related aromatic arsenic compounds. J Hazard Mater 175:352–358
19. Monasterio RP, Londonio JA, Farias SS, Smichowski P, Wuilloud RG (2011) Organic solvent-free reversed-phase ion-pairing liquid chromatography coupled to atomic fluorescence spectrometry for organoarsenic species determination in several matrices. J Agric Food Chem 59:3566–3574
20. Howie M (2005) feed additive compendium, MillerPubl. Co., Minnetonka, MN, Additives and their uses 43:125–436
21. Depalma S, Cowen S, Hoang T, Al-Abadleh HA (2008) Adsorption thermodynamics of p-arsanilic acid on iron (oxyhydr) oxides: in-situ ATR-FTIR studies. Environ Sci Technol 42:1922–1927
22. Mitchell W, Goldberg S, Al-Abadleh HA (2011) In situ ATR-FTIR and surface complexation modeling studies on the adsorption of dimethylarsinic acid and p-arsanilic acid on iron-(oxyhydr) oxides. J Colloid Interface Sci 358:534–540
23. Li P, Hu B (2011) Sensitive determination of phenylarsenic compounds based on a dual preconcentration method with capillary electrophoresis/UV detection. J Chromatogra A 1218:4779–4787
24. Liu J, Yu H, Song H, Qiu J, Sun F, Li P, Yang S (2008) Simultaneous determination of p-arsanilic acid and roxarsone in feed by liquid chromatography-hydride generation online coupled with atomic fluorescence spectrometry. J Environ Monit 10:975–978
25. Dai H, Yang CP, Ma XL, Lin YY, Chen GN (2011) A highly sensitive and selective sensing ECL platform for naringin based on beta-Cyclodextrin functionalized carbon nanohorns. Chem Commun 47:11915–11917
26. Shen Y, Zhang Y, Zhang Q, Niu L, You T, Ivaska A (2005) Immobilization of ionic liquid with polyelectrolyte as carrier. Chem Commun 33:4193–4195
27. Anson F (1964) Application of potentiostatic current integration to the study of the adsorption of cobalt (III)-(Ethylenedinitrilo (tetraacetate) on mercury electrodes. Anal Chem 36:932–934
28. Tang L, Wang Y, Li Y, Feng H, Lu J, Li J (2009) Preparation, structure, and electrochemical properties of reduced graphene sheet films. Adv Funct Mater 19:2782–2789
29. Dai H, Gong LS, Xu GF, Zhang SP, Lu SY, Jiang YW, Lin YY, Guo LP, Chen GN (2013) An electrochemical sensing platform structured with carbon nanohorns for detecting some food borne contaminants. Electrochim Acta 111:57–63
30. Ates M (2010) A comparative study of redox parameters and electrochemical impedance spectroscopy of Polycarbazole derivatives on carbon fiber microelectrode. Fibers Polym 11:1094–1100
31. Laviron E (1979) General expression of the linear potential sweep voltammogram in the case of diffusionless electrochemical systems. J Electroanal Chem 101:19–28
32. Zhang L, Zhang CH, Lian JY (2008) Electrochemical synthesis of polyaniline nano-networks on p-aminobenzene sulfonic acid functionalized glassy carbon electrode Its use for the simultaneous determination of ascorbic acid and uric acid. Biosens Bioelectron 24:690–695
33. Zhang L, Shi ZG, Lang QH, Pan J (2010) Electrochemical synthesis of belt-like polyaniline network on p-phenylenediamine functionalized glassy carbon electrode and

its use for the direct electrochemistry of horse heart cytochrome c. Electrochim Acta 55:641–647
34. Wang Y, Wang X, Li CM (2010) Electrocatalysis of Pd–Co supported on carbon black or ball-milled carbon nanotubes towards methanol oxidation in alkaline media. Appl Catal B 99: 229–234
35. Galus Z (1976) Fundumentals of electrochemical analysis. Ellis Horwood, New York
36. Raoof JB, Chekin F, Ojani R, Arari S (2013) Carbon paste electrode incorporating multi-walled carbon nanotube/ferrocene as a sensor for the electroanalytical determination of N-acetyl-L-cysteine in the presence of tryptophan. J Chem Sci 125:283–289